Estuarine, Coastal and Shelf Science 194 (2017) 97–108

Contents lists available at ScienceDirect

Estuarine, Coastal and Shelf Science

journal homepage: www.elsevier.com/locate/ecss

# Observational and numerical particle tracking to examine sediment dynamics in a Mississippi River delta diversion

Mead A. Allison [a, b, *], Brendan T. Yuill [b], Ehab A. Meselhe [b], Jonathan K. Marsh [c], Alexander S. Kolker [a, d], Alexander D. Ameen [a]

[a] Tulane University, New Orleans, USA
[b] The Water Institute of the Gulf, Baton Rouge, USA
[c] ETS, United Kingdom
[d] LUMCON, USA

ARTICLE INFO

*Article history:*
Received 21 February 2017
Received in revised form
25 May 2017
Accepted 3 June 2017
Available online 7 June 2017

*Keywords:*
Particle tracking
Sediment tracer
Numerical modeling
River diversion
Mississippi River delta
Coastal restoration

ABSTRACT

River diversions may serve as useful restoration tools along coastal deltas experiencing land loss due to high rates of relative sea-level rise and the disruption of natural sediment supply. Diversions mitigate land loss by serving as new sediment sources for land building areas in basins proximal to river channels. However, because of the paucity of active diversions, little is known about how diversion receiving-basins evacuate or retain the sediment required to build new land. This study uses observational and numerical particle tracking to investigate the behavior of riverine sand and silt as it enters and passes through the West Bay diversion receiving-basin located on the lowermost Mississippi River delta, USA. Fluorescent sediment tracer was deployed and tracked within the bed sediment over a five-month period to identify locations of sediment deposition in the receiving-basin and nearby river channel. A computational fluid dynamics model with a Lagrangian sediment transport module was employed to predict selective pathways for riverine flow and sand and silt particles through the receiving-basin. Observations of the fluorescent tracer provides snapshots of the integrated sediment response to the full range of drivers in the natural system; the numerical model results offer a continuous map of sediment advection vectors through the receiving basin in response to river-generated currents. Together, these methods provide insight into local and basin-wide values of sediment retention as influenced by grain size, transport time, and basin morphology. Results show that after two weeks of low Mississippi River discharge, basin silt retention was approximately 60% but was reduced to 4% at the conclusion of the study. Riverine sand retention was approximately near 100% at two weeks and 40% over the study period. Modeled sediment storage was predicted to be greatest at the margins of the primary basin transport pathway; this matched the observed dynamics of the silt tracer but did not match the behavior of the sand tracer. The degree to which the observational measurements deviate from the model predictions may indicate the relative influence of physical processes other than the mean riverine generated currents, such as tides, wind generated currents, and waves.



## 1. Introduction

Large river deltas are under threat worldwide in response to the effects of climate change and direct human modification of their geomorphic processes and ecosystems (Day et al., 2008; Bianchi and Allison, 2009). The vast coastal wetlands in and around deltas often support extremely productive fisheries and aquatic habitat (Boesch and Turner, 1984; Bell, 1997; Day et al., 1997) and offer inland areas valuable protection from large storms (Costanza et al., 2008). However, these wetlands are under particular threat due to very large rates of land loss (Gagliano et al., 1981; Britsch and Dunbar, 1993). This wetland loss is driven by system-wide modifications that include (1) declining sediment supply arriving from upland sources due to damming and the disruption of floodplain connectivity (Meade et al., 1990; Syvitski et al., 2007), (2) accelerating rates of eustatic sea level rise (ESLR) that can drown low elevation coastal wetlands (Blum and Roberts, 2009), (3) possible

* Corresponding author. Tulane University, New Orleans, USA.
*E-mail address:* meadallison@tulane.edu (M.A. Allison).

http://dx.doi.org/10.1016/j.ecss.2017.06.004
0272-7714/

increases in the frequency or intensity of tropical cyclones that remove wetlands through wave attack and wholesale removal of the surficial organic layer (Morton and Barras, 2011), and (4) artificial leveeing, and re-direction and closure of delta distributary channels for flood control and to improve navigation between inland and coastal waters (Syvitski and Saito, 2007). In deltaic wetlands, the problem is greatly compounded by subsidence driven relative sea level rise (RSLR) that often exceed ESLR and are caused by both natural (e.g., Holocene sediment compaction, peat oxidation) and human (e.g., geofluid withdrawal) drivers (Syvitski et al., 2009; Yuill et al., 2009; Kolker et al., 2011; Allison et al., 2016).

One potential restoration method to maintain deltaic wetlands in RSLR conditions is to divert sediment-laden water from distributary channels into the adjacent wetland basins. While water and sediment diversions from distributary channels has been practiced in a number of deltas worldwide for various purposes (see Allison et al., 2014 for examples), preservation of existing deltaic wetlands and restoration of lost wetlands in the Mississippi delta exceeds the scope of previously attempted projects. Restoration on this scale may be possible, because, as a sediment supply-dominated delta characterized by low wave and tidal energy (Roberts, 1997), the modern (<7.5 kyr) extent of Mississippi delta's wetlands has been primarily controlled by late Holocene, depositional lobe-forming processes. Reintroduction of sediment-laden river water, which mimics the natural effects of crevasse splay formation and evolution in deltas (Kim et al., 2009; Allison and Meselhe, 2010; Paola et al., 2011; Meselhe et al., 2012; Wang et al., 2014) is a major strategy proposed in the delta's ecosystem restoration plan (LACPRA, 2012).

The key elements of future distributary channel design in deltaic wetlands for land building from diverted river water are maximizing (1) the water to suspended sediment ratio in the diversion relative to the river (Meselhe et al., 2012) and (2) the retention of sediments in the receiving area. Maximizing sediment capture, particularly of the sediment (sand and coarse silt) in suspension and available for capture by a diversion will be controlled by factors such as (1) the angular orientation and intake invert elevation of the diversion channel (Gaweesh and Meselhe, 2016; Yuill et al., 2016), and (2) proximity to bank margin sand bars (lateral or point bars) that are a significant local source of bed material load (Ramirez and Allison, 2013; Allison et al., 2014).

The concentration, grain size, and timing of the sediment captured by the diversion will impact sediment retention in the receiving area—the second key element of diversions mentioned above. For example, it is more beneficial to divert relatively coarse sediment because of its faster settling velocities and enhanced resistance to resuspension. Both sand and mud are likely critical for optimizing splay deposition: sand with rapid settling and limited consolidation forms a firm substrate for initial subaerial emergence, while fines serve to sustain existing wetlands in the basin and aid in vertical accretion when subaerial areas are colonized by vegetation (Peyronnin et al., 2016). Sediment retention efficiency in the receiving basin will also be controlled by the evolution of splay islands and channels, as can be observed in the evolution of the Wax Lake delta in Atchafalaya Bay (Roberts, 1998; Shaw and Mohrig, 2014; Shaw et al., 2016). Natural splay island development is an integral part of delta growth (Wellner et al., 2005; Esposito et al., 2013) as they provide resistance to local flow and shield inland waters from waves.

The West Bay Diversion (WBD) is the only diversion constructed to date in the Mississippi River (MR) designed for the purpose of building and sustaining wetlands by mimicking the crevasse splay process. This site provides a unique opportunity to investigate the performance of an operating sediment diversion, especially as it relates to capture efficiency and sediment retention in the receiving area (e.g., West Bay [WB]; Fig. 1). The present study utilizes a novel combination of particle tracking methods to investigate sediment movement in and around the WBD. The first particle tracking method is a field-based approach that samples the abundance of a deployed fluorescent sediment tracer. While fluorescent sediment tracers have long been used in fluvial sediment tracking studies (Kennedy and Kouba, 1970), recent laboratory advances permitting quantification of the fluorescent particle content in highly diluted concentrations (grains/kg of sediment; Marsh et al., 1997; McComb and Black, 2005) allow their wider applicability today to explore the combined influence of river currents, tides, and waves on the movement of riverine sediment (see Elias et al., 2011 for an example of the combined tracer-modeling approach similar to the present study). In the present experiment, fluorescent tracer was tracked from the river channel into and through a diversion receiving basin over three discrete time periods spanning five months. The second particle tracking method utilizes a computational fluid dynamics model to simulate the transport of individual sediment grains throughout the WBD based on the predicted flow (velocity and pressure) fields due to river currents only. The objective of this study is to utilize these particle tracking methods to characterize the behavior of riverine sediment as it passes through the WBD focusing on identifying preferred transport pathways and estimating areas of retention. The time window of analysis was kept short to increase the probability that a significant fraction of the fluorescent tracer was recovered and to minimize the amount of morphological changes that could occur within the basin relative to static bathymetry used in the model. The modeling component of this study was expanded to test how a set of engineered sand islands constructed within the receiving basin altered the predicted flow field and how, in turn, the altered flow field might have influenced basin sediment retention.

## 2. Study area

The WBD is an uncontrolled (earthen) diversion channel cut through the right descending bank of the MR at a point 7.6 km above the Head of Passes final bifurcation of the river channel (RK7.6; Fig. 1). The diversion was designed to renew a natural crevasse splay that was formed in 1838 and by the late 20th century had subsided and eroded into an open bay setting (i.e., West Bay) bounded by the MR bankline and remnant natural levees associated with natural Grand Pass (Coleman and Gagliano, 1964; Andrus, 2007). Completed in November 2003, the initial cut (59.4 m wide, 7.6 m deep) was designed to discharge an initial flow rate of 20,000 cfs (566 $m^3/s$) at the 50% duration stage of the MR. It was intended to be mechanically enlarged to a 50% stage duration flow rate of 50,000 cfs (1416 $m^3/s$) of the MR at Venice, Louisiana (Fig. 1) two to three years later if there was no evidence of thalweg capture (Sharp et al., 2013). While this mechanical enlargement was never carried out, the diversion cut self-evolved to 204 m wide with an average depth of 12.8 m depth by 2014 (Yuill et al., 2016). The Yuill et al. (2016) study documents how discharges through the diversion cut at moderate MR flow (15,600 $m^3/s$) peaked in 2009 at about 1200 $m^3/s$, and declined in the 2009–2014 period to about 700 $m^3/s$ in spite of the increased cut cross-sectional area and hydraulic radius, likely due to increasing receiving basin bed elevation.

Bathymetric surveying in WB has shown that after an initial period of elevation loss, likely attributable to the passage of Hurricane Katrina in 2005 (Andrus, 2007), sediment accumulation has outpaced relative sea level rise (RSLR) causing shoaling. Kolker et al.

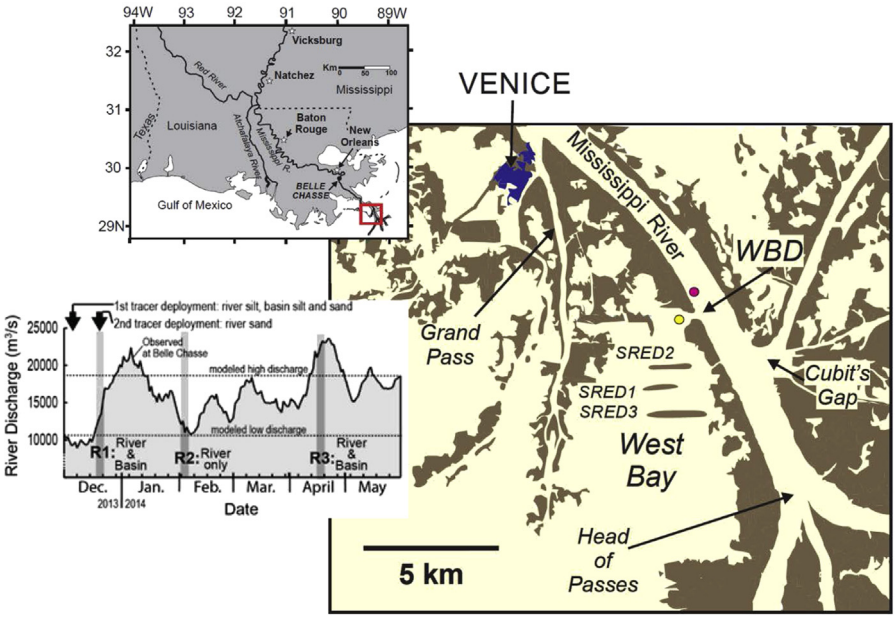


**Fig. 1.** Map of the study area showing the location of the West Bay Diversion (WBD) from the Mississippi River, the town of Venice, Louisiana, and the Sediment Retention Erosion Device (SRED) islands emplaced in the West Bay receiving area in the order (1, 2, 3) of their construction. Dark areas are land and light areas water. The circles represent the deployment points of the fluorescent tracer in the Mississippi River (purple) and in WBD (yellow). Lower inset shows daily Mississippi River water discharge at the U.S. Geological Survey station at Belle Chasse, Louisiana with the timing of the fluorescent tracer deployments (arrows) and the rounds (R) of surficial bed sampling for tracer concentrations (gray rectangles). Also shown are the modeled discharges used in this study. (For interpretation of the references to colour in this figure legend, the reader is referred to the web version of this article.)

(2012) utilized particle-reactive radiotracers to examine cores collected in WB in 2009 and found that >1 cm was deposited in summer 2009 ($^{7}$Be deposition rates) and up to 20 cm of sediment was deposited between 2003 and 2009 ($^{137}$Cs accumulation rates). While they also estimated that these rates match or exceed low-end estimates of RSLR specific to WB and fall short of maximum estimates, events after 2009 have shown the basin is shoaling. Splay islands became emergent in WB (USACE, 2012) following the large MR flood of 2011 (Khan et al., 2013). In late 2009, oblong islands were constructed in WB by Federal and local authorities using pipe-lined dredge spoil from navigational dredging of the adjacent MR thalweg navigation channel. Locally referred to as Sediment Retention Erosion Devices (SREDs), these islands were envisioned to increase trapping efficiency by reducing water velocities for flow emerging from the WBD, and to limit wave fetches that may generate resuspension. Even though performance of the SRED's in WB has not been systematically evaluated to date, two additional SRED lines (see Fig. 1) were constructed between 2012 and 2014, prior to the present field experiment.

In addition to providing a beneficial use for river dredge spoil, dredging volumes necessary to maintain navigation channel depth and width in the MR reach opposite WB and immediately upstream of Head of Passes (Pilottown reach) have increased since the construction of WBD. An extensive study of the Pilottown MR reach (Sharp et al., 2013) concluded that a combination of factors has led to the progradation of the right lateral bank sand bar (through which the WBD was cut) into the navigation channel and thalweg shoaling. The causal factors include stream power loss associated with the water loss through WBD, as well as deepening of the navigation channel and upstream passes (e.g., Baptiste Collette and Grand Pass) in the 1970s and 1980s. The present experimental and modeling study encompasses the reach of the MR river adjacent to WB as well as the WB receiving area because of this demonstrated coupling between the efficiency of sediment capture by WBD and evolving MR morphology immediately downstream.

## 3. Methods

### 3.1. Particle tracking using fluorescent sediment tracers

The tracer particles used in this study were manufactured using a thermoplastic polymer base with a particle density of 2.65 g cm$^{-3}$ infused with a fluorescent dye. Tracer particles were made in sand and silt particle size classes. Four fluorescent sediment tracer releases were conducted within the study area. On December 5, 2013, two 50 kg tracer masses infused with yellow fluorescent dye (one sand-sized tracer mass and one silt-sized tracer mass) were deployed within the receiving area at approximately 5 m water depth. On the same date, one 50 kg mass of silt-sized tracer infused with purple fluorescent dye was deployed on the right descending bank lateral sand bar in the Mississippi River at approximately 6 m water depth. On December 18, 2013, an additional 50 kg mass of sand-sized tracer infused with purple fluorescent dye was released in the MR at the same site as the previous 'purple' silt-sized tracer release. The approximate deployment locations are shown in Fig. 1. The particle-size distributions for the deployed tracer masses are shown in supplementary Fig. 1 (Figure S1). The median grain sizes of the sand tracer masses were 339 (Yellow) and 283 μm (Purple). The median grain sizes of the silt tracer masses were 10.1 (Yellow) and 9.0 (Purple) μm.

Bed sediment sampling to examine the dispersal of the silt and sand tracers was conducted in the WBD receiving area and the adjacent MR on December 16–19, 2013 (Round 1), February 3–7, 2014 (Round 2), and April 17–20, 2014 (Round 3). Detailed explanation of particle characteristics, as well as deployment bed sampling methods can be found in the online supplementary material (OSM).

### 3.2. Particle tracking using numerical simulation

The role of surface water hydrodynamics in driving sediment

transport within the study area was examined using numerical simulations. Simple steady-state river discharges were modeled to calculate preferential sediment transport pathways and zones of apparent sediment accumulation within the study area. An objective of these numerical experiments was to simulate 'typical' flow (i.e., velocity and pressure) fields in river water as it entered and passed through a sediment diversion and its receiving-basin to investigate how these fields may or may not be responsible for the observed sediment tracer displaced through the study period. In these experiments, the flow fields are the product of a prescribed river discharge and the effects of the modeled receiving basin morphology and the effects of wind, waves, tides, and other allogenic influences were explicitly not simulated.

River flow was simulated using a mature computational fluid dynamics (CFD) modeling suite that solves the three-dimensional, transient Naiver-Stokes equations of fluid motion (i.e., Flow-3D; www.flow3d.com). The CFD model simulated sediment transport using a Lagrangian mass particle tracking approach.

The model experiments simulated two steady-state discharges, 10,500 and 18,000 $m^3/s$ which are approximate to the low and high river discharges within the observational study period. The modeled sediment particles' diameters were set as the observed median diameters of each tracer specie deployed at the river and diversion channel location, i.e., silt and sand. Sediment particles were randomly fed into the river reach upstream of the diversion inlet at a steady rate; the transport patterns of the particles through the study area were measured once steady-state transport fields were achieved. In addition to simulating the low and high discharge within the observed bathymetry (the '*obsBathy*' scenarios) model simulations, two more (low and high) discharge simulations were executed with a modified receiving-basin bathymetry that replaced the SRED island topography with elevation values from the surrounding basin bed (the '*noSREDs*' scenarios). These simulations were executed to test the influence of the SRED islands on the sediment transport storage and pathways within the receiving basin.

The numerical methods employed by this study are described in greater detail in the OSM.

## 4. Results

### 4.1. Observations from the fluorescent particle tracer field experiment

The observed distribution of fluorescent tracer silt and sand from the river (Purple) and receiving basin (Yellow) deployment sites and the subsequent bed material sampling sites are shown in the supplementary material (Figs. S2, S3). Because of the much larger counts in the silt experiment, these are expressed hereafter in counts/$cm^2$ (e.g., Fig. S2), while sand experimental results are shown in counts/$m^2$ (e.g., Fig. S3). Fig. 1 (inset) shows the discharge conditions in the MR during the experiment. The 11–13-day period between deployment of the Yellow sand and silt and the Purple silt, and the Round 1 sampling, was marked by low river discharges (mean 9670 $m^3/s$). The subsequent 46 days until the beginning of Round 2 sampling (river only) was marked by rising river discharge to a peak on January 6th (22,400 $m^3/s$), before falling to about 11,000 $m^3/s$ at Round 2 sampling. Between Round 2 and 3 (69 days), the MR was generally in a rising discharge trend, reaching a peak at the time of Round 3 sampling (23,300 $m^3/s$).

In Round 1 (low river discharge), the receiving basin-deployed Yellow silt was observed to have distributed basin wide (Fig. S2 upper left), with the highest counts/$cm^2$ concentrated along the deeper western side of WB, although sampling was limited in the shallow southeastern portion of the bay. None of the Yellow silt was observed to have moved into the MR. The Purple silt deployed in the MR (Fig. S2 lower left) displayed a similar Round 1 pattern in the receiving basin, indicating capture of fine MR sediments by the WBD, and was found at the highest concentrations in the MR in the thalweg along the left descending bank. In Round 1, the Yellow sand (Fig. S3 upper left) showed limited dispersal from the immediate vicinity of the deployment location. No sampling of the Purple sand was possible since it was deployed immediately after completion of the Round 1 sampling.

After the first river discharge peak, a limited bed sampling campaign was conducted in the MR with no WB sampling (Round 2) and the Purple sand was deployed at the MR site. Unlike Round 1, the Yellow silt showed significant advection of fines was taking place into the MR (Fig. S2, upper center). Although MR sample locations are slightly different, Purple silt concentrations and distribution (Fig. S2, lower center) were similar to Round 1. Unlike the Yellow silt, the Yellow sand showed no evidence of advection into the MR (Fig. S2, upper center). The Purple sand displayed limited evidence of downstream MR advection from the deployment site (Fig. S3, lower center) despite the relatively high flow event in early January.

The final sampling of the tracers (Round 3) in April 2014 after a more extended period of rising to high MR discharge, shows distinct changes in tracer distribution from the first two sampling periods. The Yellow silt (Fig. S2, upper right) showed continued presence in the MR but a reduction in basin wide concentration in WB (accounting for the differences in sampling site), with greater evidence of reduced concentrations in the shallow eastern part of the receiving basin relative to the western. The Purple silt (Fig. S2, lower right) showed a similar MR concentration and distribution to the Yellow silt, but these values are reduced from those observed in Rounds 1 and 2. In WB, the Purple silt distributions are similar (focused in the western receiving area) to the Yellow silt and are also reduced relative to Round 1, but less so than the Yellow silt. The Yellow sand (Fig. S3, upper right) and the Purple sand (Fig. S3, lower right) both show limited concentrations in the MR downstream of the deployment site. Both sand tracers now show significant dispersal into WB, although the highest concentrations are still found in the upper portion of the bay.

### 4.2. Bed grain size

The surficial sediment grain size measurements conducted on samples collected at the time of the three rounds of fluorescent tracer sampling showed a wide variation from clayey silts to fine sands, with a median ($D_{50}$) grain sizes ranging from 5.1 to 227.3 μm. Fig. 2 plots of sand content in the low discharge (Round 1) sampling exhibit a heterogeneous distribution of muds and sands in the WB receiving area other than the SRED islands are >95% sand. The thalweg of the MR channel, which trends near the left descending bank, showed relatively muddy conditions were present in this round, while sands were present on the right descending bank lateral bar. After the first discharge peak (Round 2), the limited dataset in the MR (Fig. 2) displays no clear trend. In the more substantial sampling in Round 3 at the second peak in MR discharge, the river thalweg is significantly sandier, while the receiving area in WB displays a heterogeneous distribution with a similar spatial pattern to Round 1grain size trends.

### 4.3. Results from numerical modeling

Fig. 3 shows relative values of the predicted sediment particle density at steady state averaged over the area of each polygon used to analyze bed sediment texture (initially defined in Fig. 2). Relative sediment density was quantified as $P^*$ which is defined as the

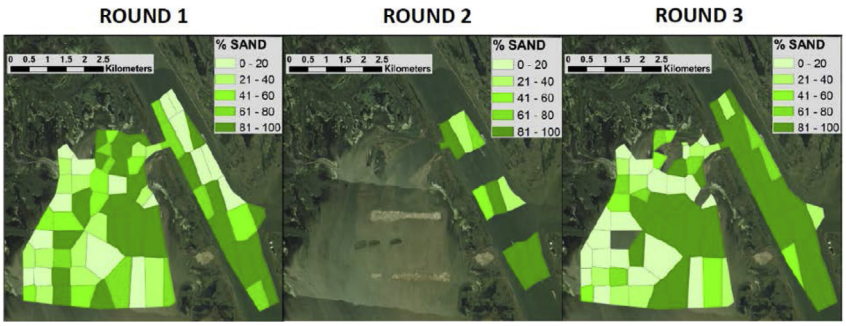


**Fig. 2.** Percentage of sand in surficial bed samples as measured at the time of the three rounds of sampling for the fluorescent tracer in the West Bay receiving area and adjacent Mississippi River. Sample locations were averaged to the Thiessen polygons (boundaries define the area that is closest to each point relative to all other points) to aid in tracer mass budget calculations.

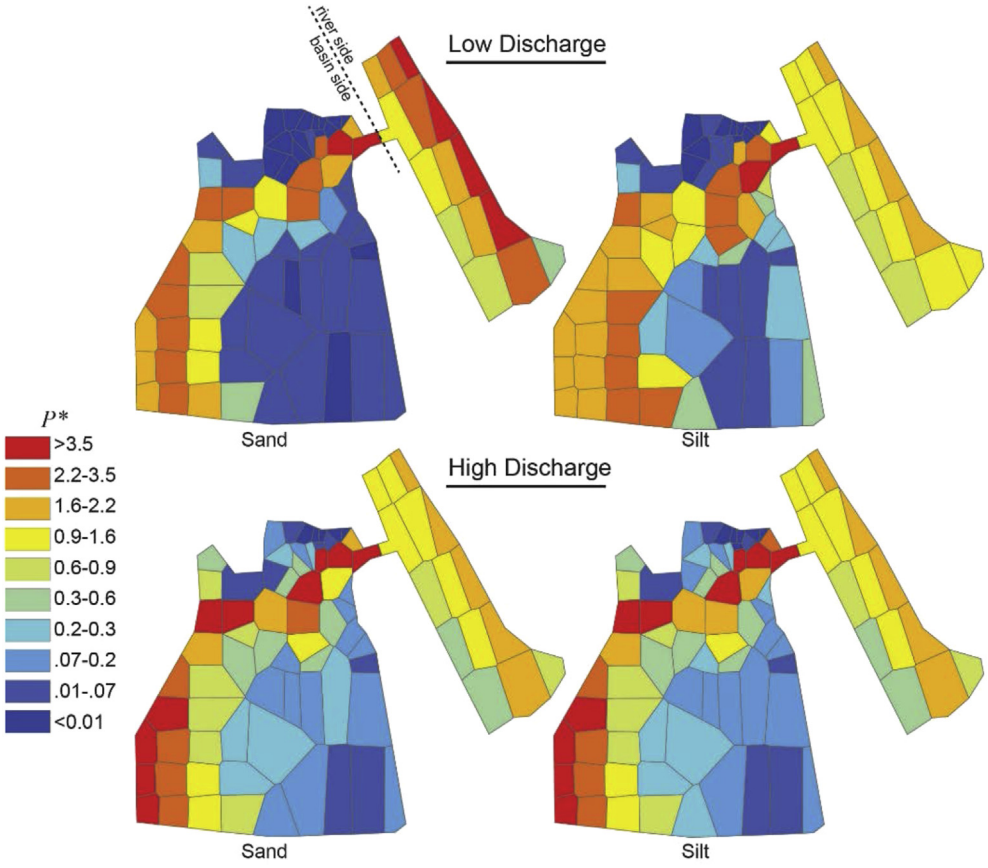


**Fig. 3.** Relative particle density at steady-state calculated during the *obsBathy* simulations.

number of sediment particles per square-meter (p/m$^2$) divided by the mean particle density for the larger bounding geomorphic regions. The two larger geomorphic regions considered are the extents of the river channel and the receiving basin within the model domain. For the high-discharge model scenario, the predicted spatially-averaged sand density was 0.073 p/m$^2$ in the river channel and 0.013 p/m$^2$ in the receiving-basin; the predicted spatially-averaged silt density was 0.073 p/m$^2$ in the river channel and 0.010 p/m$^2$ in the receiving-basin. For the low-discharge scenario, these values were 0.130 p/m$^2$, 0.009 p/m$^2$, 0.100 p/m$^2$, and 0.011 p/m$^2$ respectively.

Relative to the *obsBathy* scenarios, the flow and sediment transport velocity magnitudes and sand and silt particle abundances were greater in the scenarios with the engineered SRED islands removed (i.e., the *noSRED* scenarios) (Fig. 4). The flow and sediment pathways were more diffused throughout the basin with the absence of the SREDs; however, the sediment was still preferentially steered into the western section of the receiving-basin.

See OSM for auxiliary detail on modeling results.

## 5. Discussion

### *5.1. Pathways of sediment dispersal and trapping efficiency as indicated by the tracer experiment*

Thiessen polygons, in which the boundaries define an area that is closest to each point relative to all other points (Thiessen, 1911), were used to determine particle concentrations as normalized to

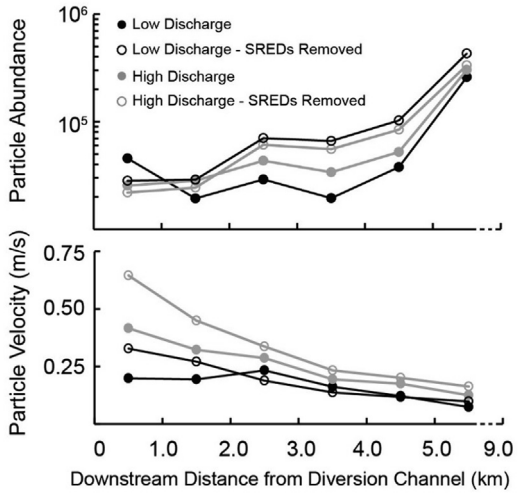


**Fig. 4.** Modeled (at steady-state) sand particle abundance and spatially-averaged sand particle velocity through the receiving basin at 6 spatial intervals. Model results are shown for the high and low discharge scenarios, with and without the SRED islands incorporated in the modeled bathymetry.

the grain size of the sample (Fig. 2). Thiessen polygons were determined from Round 1 sampling locations in the MR and WB receiving area because this was the largest number of samples. To account for the fact that some Round 2 and 3 sample sites were in different locations than Round 1, the normalized number of particles/cm$^2$ were determined when a Round 2 or 3 sample site fell in a specific Round 1 polygon: averages were utilized when multiple samples fell in a Round 1 polygon.

Figs. 5 and 6 show normalized tracer concentrations determined from the granulometry that were calculated by multiplying the observed total by the fractional percentage of the sample with that grain size class (sand or silt). The purpose of this calculation was to allow spatial trend comparisons after removing the effects of grain size. The resulting normalized spatial trends of the tracers do not display dramatic differences from the non-normalized values (Fig. S2 and S3), but can be utilized to calculate mass tracer particle budgets using the total number of particles deployed at each site (Purple and Yellow) for the sand and silt tracers to scale up from number of particles in a grab sample (20 × 20 × 2 cm) to total particle numbers in each polygon area (to a sediment depth of 2 cm). The limited sampling area in Round 2 did not allow for a mass budgeting.

The tracer experiment mass budgets are shown as sums for various sub-areas of the study area (outlined in Figs. 5 and 6) in Table 1. Several conclusions about the retention efficiency of the MR and WB receiving area can be made from this budget. After approximately two weeks of low discharge conditions (Round 1 sampling), 60.1% of the WBD deployed silt (Yellow) can be accounted for in the receiving area and 60.0% of the MR deployed silt (Purple) was also retained within the receiving area. This suggests that (1) bottom shear stresses in the MR and WB were sufficient to mobilize the bulk of the finer tracer particles and (2) that the deployment site of the Purple silt was sufficiently close to the right descending bank of the MR that much of the water into which this silt was entrained was captured by WBD (only 17.2% of the Purple silt was found in the MR channel). More tracer silt from both sources was found in the Lower WB area than near the WBD. By Round 3 after several high MR discharge events, only 3.4% of the Yellow and 6.5% of the Purple silt could be accounted for in the WB receiving area. Only a small fraction of this reduction is due to a reduction in the grid area sampled (Fig. 5). While this reduction between Round 1 and 3 sampling likely indicates flushing of the majority of the tracer silt out of the study area (out of WB and further down the MR channel), it is not possible to differentiate loss from the study area from burial below the depth of sampling (2 cm) or sediment that remained immobile at the deployment point.

After low discharge conditions when Round 1 sampling was conducted, only 27.9% of the WBD deployed sand (Yellow) could be accounted for in the mass budget (Table 1). While this is likely related to the bottom shear stresses being insufficient to resuspend the sand-sized tracer, and hence, the majority of the tracer remained in close proximity to the deployment site if bedload transport is the only active transport mechanism, burial or immobility is also a possibility. Loss from WB receiving area is unlikely given all the Yellow sand is concentrated in Upper WB. By Round 3 sampling, 39.5% of the Yellow sand could be accounted for—38.9% in the WB receiving area and 0.6% that was advected into the MR, likely through tidal reversals in flow. The majority of the Yellow sand in the receiving area was in Lower WB, indicating it had been transported beyond the SRED islands and is unlikely to remain and be buried in WB given its progressive vector and passage beyond the SRED barriers to release from the basin. The Purple sand released at the time of the Round 1 sampling into the MR, showed limited movement downriver or into WB after the first high flow event (Round 2; Fig. 6). By Round 3, 17.4% of the Purple sand was accounted for—all of it in WB. This history of the Purple sand supports the concept observed in the Purple silt of high efficiency of capture of particles from the MR deployment site into WBD.

The relative importance of bedload versus suspended sand transport in these results can be inferred from the peak MR discharges reached (Fig. 1 inset). Peak discharges in the high flow event before Round 2 reached 22,000 m$^3$/s and 23,000 m$^3$/s in the second event before Round 3. Ratings curves at Belle Chasse (RK122) suggest suspended sand levels are negligible below about 12,000 m$^3$/s in the lowermost MR (Allison et al., 2013), while isokinetic and backscatter studies on the bar at Myrtle Grove, Louisiana (RK91) show significant resuspension of bed material load takes place beginning at about 19,000 m$^3$/s (Ramirez and Allison, 2013). The offset in these values may be due to the presence of finer sand transported as washload from the catchment. Flow at WB is reduced from that measured daily at Belle Chasse, however, due to the loss of water through cuts between these points in the MR (e.g., Bohemia Spillway, Ostrica, Ft. St. Phillip, Baptiste Collette, Grand Pass). Using annual water budgets in Allison et al. (2013) suggests that these cuts are responsible for about a 28% loss in MR flow, which would reduce the flow in the peaks observed in Jan.–April 2014 below that observed to generate significant resuspension of bed material load in upriver bars. Several studies in this MR reach (Nittrouer et al., 2008; Ramirez and Allison, 2013) have shown that while sand loads transported by bedform transport increase exponentially with flow, smaller bedforms are transporting sand downriver even at flows observed in Round 1–3 MR discharges.

It is clear from the mass budgeting exercise (Table 1), that definitive statements about (1) the relative importance of burial below sample depth by bed aggradation and dune migration, and (2) immobility at the deployment site versus transport out of the sampled area cannot be ascertained from the tracer experimental results. The remaining sections utilize the numerical results to gain additional insight into how these processes impact the efficiency of capture within the WB receiving area.

### 5.2. Comparison of the simulated sediment dynamics to the observational tracer results

The model results shown in Fig. 7 illustrate the predicted

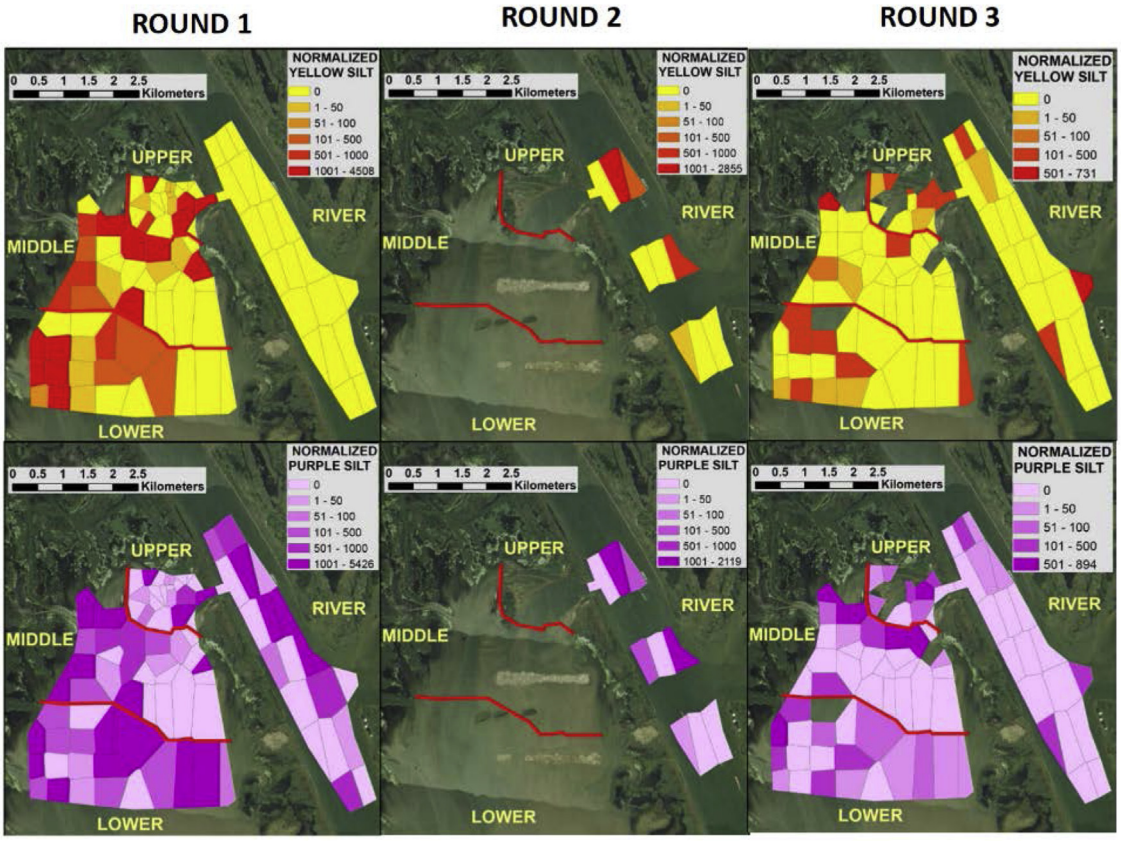


**Fig. 5.** Distribution maps of normalized fluorescent tracer silt concentrations (per cm2) in surficial sediments (0–2 cm depth interval) recovered in the West Bay receiving area (Yellow) and adjacent Mississippi River channel (Purple) in the 2013–2014 experiment. Left panels show distributions on December 16–19, 2013 (Round 1), middle panel on February 3–7, 2014 (Round 2), and right panels on April 17–20 2014 (Round 3). Boundaries for the Upper, Middle, and Lower portions of West Bay receiving area are outlined with red lines. (For interpretation of the references to colour in this figure legend, the reader is referred to the web version of this article.)

distribution of diverted riverine sediment due to river-generated currents. The figure shows snapshots of a time-independent steady-state transport field, and so are relative to sediment abundance scales with gradients in sediment particle velocity and sediment supply. For the high river discharge simulation, the distribution of sand particles was very similar to the distribution of silt particles suggesting that the selective transport pathways and relative particle velocities were independent of grain size for the range of particles considered in this study (8.9–339 μm). For the low river discharge simulation, the difference between the distributions and abundances of the sand and silt fractions became more pronounced, likely due to the divergence in the ratio of shear stress borne by each particle to the critical shear stress for each particle-size fraction. Recent analyses by Shaw and Mohrig (2014) have also indicated that spatial patterns of sediment transport and deposition within interdistributary basins can vary widely dependent on the relative magnitude of the channel flow entering the basin.

The modeled distribution of silt particles compares very favorably to the distribution of observed silt tracers (discounting the river sample sites) during the first round of sampling (in mid-December 2013). Areas of relatively high abundance for the simulated particles and the silt tracer appear at the margins of the main southerly current. The model suggests that high relative levels of silt abundances shift from being more associated with the easterly margin to the westerly margin with increasing discharge. In later sampling rounds, the relative abundance of the fluorescent silt tracer appears more random and became disassociated with the model predicted currents suggesting that other transport processes, such as tidal and wind-wave driven circulation, created a more diffuse depositional pattern.

Patterns of the observed sand sediment tracer in each sampling period in the WB receiving basin were not well correlated with the modeled sand transport dynamics. The observed distributions of the sand tracer were likely influenced by a slow transport velocity that was inadequate to distribute the tracer particle mass to the distal regions of the study area within the limited study period. Also, unlike the distribution of modeled sand particles, the observed relative abundance of sand tracer appears spatially decoupled from the predicted pathway of the primary current; abundant sand tracer was observed in the lower eastern section of the receiving-basin around the location of the SRED islands. The presence of relatively high sand tracer abundances in areas away from the primary current may have been influenced by infrequent, high magnitude events such as very-high river discharges (e.g., the hydrograph peaks occurring in early January 2013 and mid-April 2014) and frontal storms (~5 storms occurred over study period with winds > 32 km/h, rainfall > 25 mm/day) which could have created alternative currents resulting in advective pathways not captured in the model. Research by Roberts et al. (2015) found that relatively frequent, moderate-sized storms (e.g., cold fronts) can redistribute and trap significant fractions of sediment within a receiving basin providing that the storm surges the water level above the local marsh surface. The model predicts (Fig. 7, S13) that minor currents are increasingly steered into the eastern side of the basin with increasing river discharges. It is also possible that sand tracer was selectively transported within the primary current but

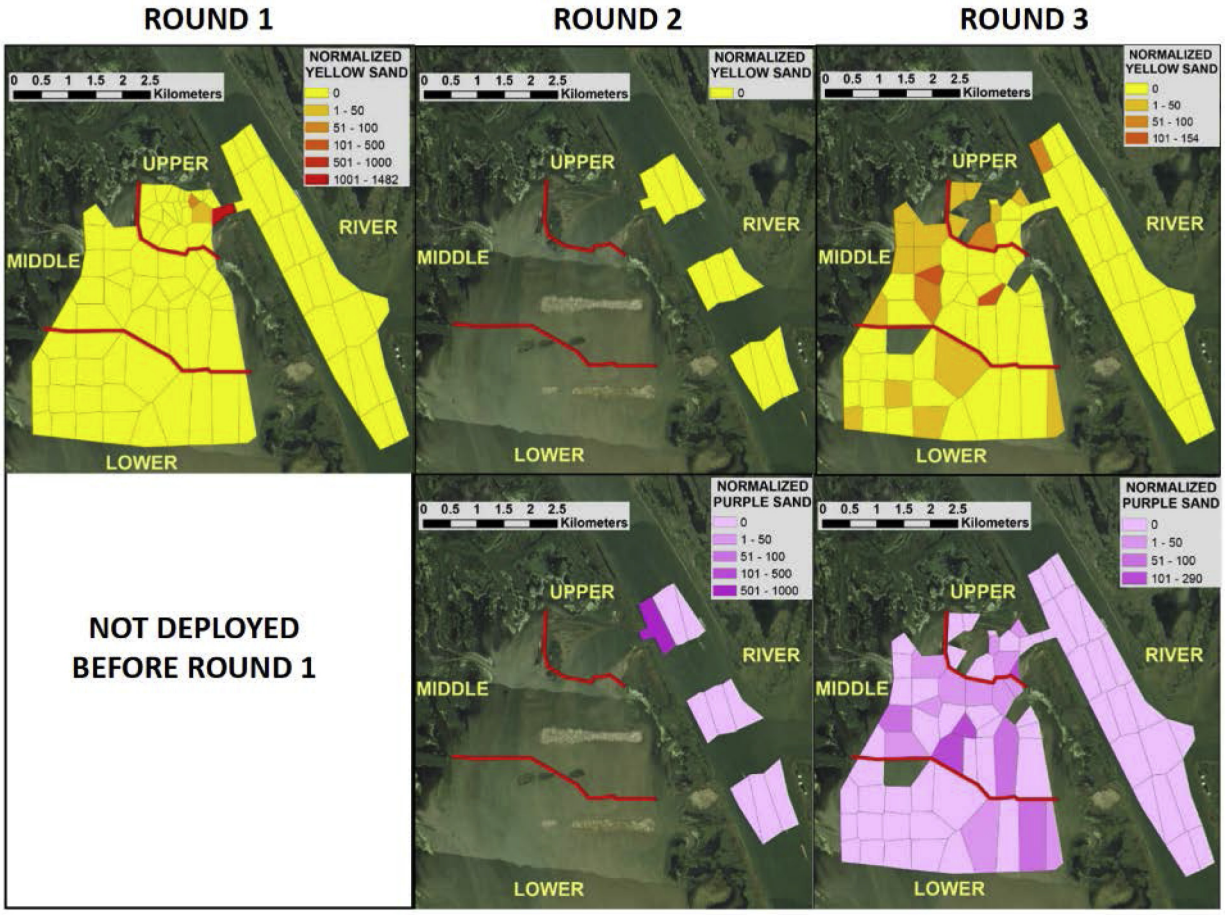


**Fig. 6.** Distribution maps of normalized fluorescent tracer sand concentrations (per cm2) in surficial sediments (0–2 cm depth interval) recovered in the West Bay receiving area (Yellow) and adjacent Mississippi River channel (Purple) in the 2013–2014 experiment. Left panels show distributions on December 16–19, 2013 (Round 1), middle panel on February 3–7, 2014 (Round 2), and right panels on April 17–20 2014 (Round 3). Boundaries for the Upper, Middle, and Lower portions of West Bay receiving area are outlined with red lines. Note that there is no information for the Purple sand in Round 1 because that tracer was not deployed until December 18, 2013 (the other tracers were released on December 5th). (For interpretation of the references to colour in this figure legend, the reader is referred to the web version of this article.)

**Table 1**
Tracer grains deployed and percentage of grains accounted for in each sub-area of the sampled reach for the Round 1 and Round 3 sampling.

| Location | Deployed Tracer Particles | | | | Round 1 | | | Round 3 * | | | |
|---|---|---|---|---|---|---|---|---|---|---|---|
| | Y M | P M | Y S | P S | Y M | P M | Y S | Y M | P M | Y S | P S |
| BASIN | grains x $10^{11}$ | | | | % | | | % | | | |
| *Upper* | 2120 | 0 | 0.017 | 0 | 9.8 | 4.0 | 27.9 | 0.6 | 0.8 | 2.7 | 1.1 |
| *Middle* | 0 | 0 | 0 | 0 | 28.1 | 23.7 | 0 | 0.9 | 3.6 | 5.7 | 10.6 |
| *Lower* | 0 | 0 | 0 | 0 | 22.3 | 31.2 | 0 | 1.9 | 2.1 | 30.5 | 5.8 |
| RIVER | 0 | 2820 | 0 | 0.021 | 0.0003 | 17.2 | 0 | 1.6 | 1.2 | 0.6 | 0 |
| TOTAL | 2120 | 2820 | 0.017 | 0.021 | 60.1 | 76.2 | 27.9 | 5.1 | 7.7 | 39.5 | 17.4 |

Y = yellow, P = purple, M = silt, S = sand; *Round 3 results do not include all polygon areas sampled in Round 1. Upper Basin % results are for 68.5% of the total Round 1 area, Middle Basin is 97.7%, Lower Basin is 95.0%, and River is 100%.

was not sampled due to burial below sampled depths (>2 cm).

The model finding that sand deposition is focused toward the margins away from the predicted pathway of primary current, doe corresponds with recent research which found that deposition at current (or jet) margins increases relative to central, downstream locations (e.g., mouth bars) in the presence of turbulent diffusivity generated by significant bed roughness (Rowland et al., 2009; Canestrelli et al., 2014) and oblique wave attack (Nardin and Fagherazzi, 2012). Further, Mariotti et al. (2013) found that, in cases where there are significant horizontal eddies in the main current, the ratio of the eddy velocity to the sediment fall velocity could also promote deposition at currents margins relative to central locations. The model results do not suggest the presence of deposition that could ultimately produce a centrally located splay deposit (typically expected within 10 diversion channel widths of the diversion outlet) despite the constriction of flow depth as the channel flow enters the basin (Edmonds and Slingerland, 2007).

### 5.3. Predicted sediment storage within the study area based on numerical modeling

Theoretically, areas experiencing high rates of sediment storage require steep, negative gradients in flow velocity, which serves as a proxy for sediment transport capacity, and high rates of upstream

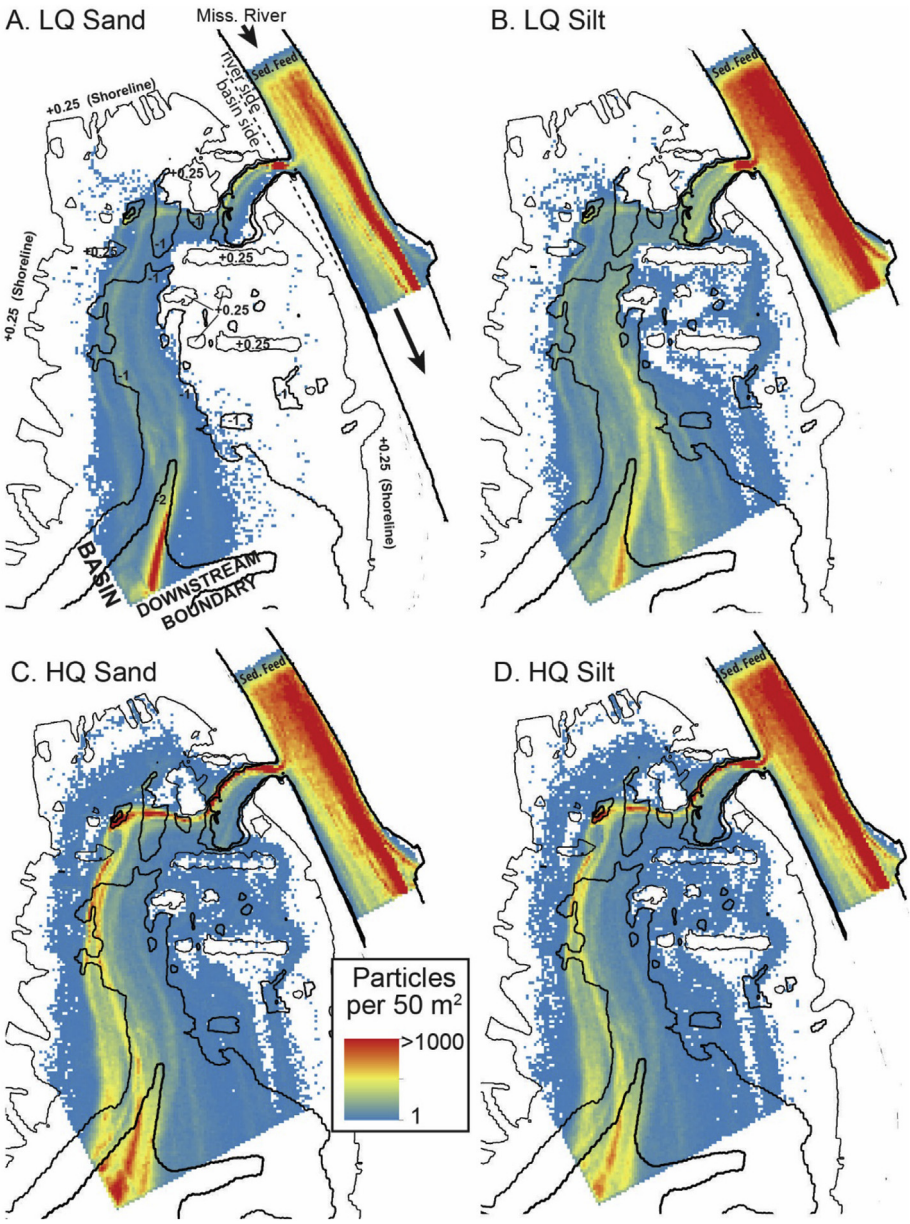


**Fig. 7.** Calculated particle density at steady-state for the *obsBathy* simulations. Each plot is at the same scale and shows data over the same model domain. Basin areas with high sediment abundances are assumed preferential for sediment accumulation.

sediment supply (Leeder, 2009). Fig. 8 shows the explicit calculation of mean velocity gradients expressed as relative values averaged over the polygons used to analyze the tracer concentrations. At the resolution shown in this figure, the steepest velocity gradients are located in the upper receiving basin where the swift moving river water mixes with the more tranquil basin water and along the western bank of the river channel. These distributions of velocity gradients would promote sediment deposition within the upper basin relative to down-basin areas; however, this trend is not evident from modeled distribution of sediment particle abundance (or in the fluorescent tracer dataset). This is likely because flow velocity gradients do not carry information about sediment supply which, as stated previously, is a required ingredient of sediment deposition. Further, the polygon boundaries were based on a sampling grid and are not aligned with specific basin geometries that may locally alter flow velocities. Prominent areas of flow acceleration or deceleration may be divided over multiple polygons, which would smooth the flow gradient over a large area. This could mask the local effect of the velocity gradient on the sediment dynamics because the sediment transport rate is nonlinearly related to flow velocity. Analysis of particle velocities indicates that sediment storage would primarily occur along the right-hand side (from a looking downstream perspective) of the primary flow current. The highest local rates of sediment deposition would likely occur in the upper basin but significant deposition would also be projected to occur along the full extent of the western margins of the basin.

### *5.4. The effect of the SRED islands on receiving-basin sediment transport*

As simulated by the numerical model, the removal of the SRED

island super-elevation from the model bathymetry increased predicted flow velocities within the diversion channel and the receiving basin. This led to a net increase in sediment transport rates within the receiving basin and a drop in predicted sediment storage. The removal of the SREDs led to a significant alteration of the river-generated currents passing through the receiving-basin. The current became more diffuse, and oriented through the central region of the basin. The primary sediment transport pathways were less responsive to the change in bathymetry and were still primarily located along the western margins of the current. The current itself, in terms of velocity magnitude and direction, did not appear to differentially push sediment towards the western side of the basin relative to the eastern side; the sediment pathway response was likely an artifact of the deeper basin waters that occupied the western basin even after the SRED islands were removed. It should be noted that subaerial land in West Bay emerged on the north and west of the core of the diversion's current in late 2011, approximately two years after the creation of the SREDs and shortly after the 2011 large flood events in March and May of that year.

Please see the OSM for additional figures illustrating the *noSRED* scenario model results.

## 6. Conclusions

This study utilized fluorescent tracer particles and numerical simulations to investigate the sediment dynamics of a Mississippi River sediment diversion receiving basin. The two methods are not substitutes for each other and do not measure the same dynamics. A synthesis of the two methods (as in Elias et al., 2011) does, however, provide a relatively robust illustration of the distribution of flow and sediment pathways and depositional zones at the transition of a laterally-confined distributary channel and an unchannelized delta front.

The observations of the fluorescent silt tracer dynamics showed that the Mississippi River and West Bay receiving basin were efficient (e.g., 99% in river, 95% in receiving basin) in rapidly (i.e., within a single water year) flushing these smaller particles beyond the sampled area. This suggests that, even with the presence of sediment retention berms (i.e., the SRED islands), Mississippi River-derived silt-size sediment is currently not a significant contributor to land building within the receiving basin. Fine sediment retention would likely increase in newly developed sand splays after they were colonized by marsh grasses. Numerical modeling suggests that, when sediment transport is primarily driven by river-generated currents discharged at the point on the river adjacent to a sand-rich lateral bar sediment source, the majority of the sediment deposition takes place along the lateral margins of the primary current where the swift, riverine sediment laden current mixes with the more tranquil basin waters.

During relatively high river discharges, the modeled current through the receiving basin was strong enough to advect the majority of both sand and silt (using the same approximate pathways) out of the receiving basin. At relatively low river discharges, the dynamics of sand and silt transport within the receiving basin were significantly different and over 90% of each size class passing through the diversion was, at least temporarily, stored within the basin. Future research is required to explore the somewhat contrasting fate of silt and sand-sized particles predicted by the two alternative particle tracking methods used in this study (i.e., the fluorescent tracer versus numerical modeling). In particular, the ability to trap fine sediment is likely very influential on the success of land building for restoration in the Mississippi Delta given the predominance of fine sediment load carried by the river.

Modeling scenarios that removed the SRED islands from the receiving-basin bathymetry predicted that flow and sediment transport rates increased relative to the observed bathymetry, which decreased net sediment storage within the basin over the modeled time period. The removal of the SREDs altered the main flow current but affected the sediment pathway less significantly. This suggests that future sediment diversions from the Mississippi River for delta restoration might benefit from a combined strategy utilizing river dredged material to construct SRED islands in the receiving area to increase sediment trapping efficiency of various particle size classes.

Generally, the fluorescent tracer data suggest that the riverine sediment becomes more equitably distributed throughout the receiving basin than indicated by the numerical model results. It is likely that this difference is due to the fact that the tracer distributions assimilate a variety of forcing mechanisms (e.g., tides and wind-wave currents) beyond river-generated currents. Further, the numerical model predicted sediment dynamics at steady-state while the fluorescent tracer results were time dependent; the fluorescent tracer particles may not have reached certain sampling locations (or were buried below sampling depth) before the sampling occurred. The model results best correlate to the distribution of silt-sized fluorescent tracer after the first round of sampling (after 2 weeks). This period may have been long enough to have permitted the silt particles to have been advected through the study area by river-generated currents, but short enough to not include many other possible influential events such as storms or cold fronts. The larger implications of these results are that river diversions in the Mississippi Delta or elsewhere will be more difficult to predict in their evolution and land-building potential if placed in the lowermost reach of the system adjacent to the ocean interface where tides and open-bay environments (e.g., strong fetch and ocean wave component) are energetic. Diversions further upriver in restricted interdistributary areas of degraded wetlands will likely have much higher trapping efficiencies.

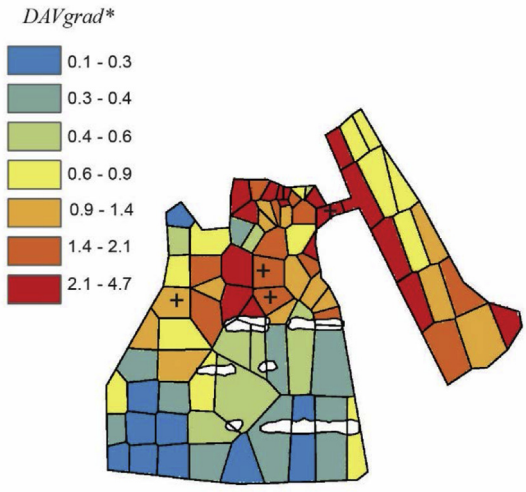


**Fig. 8.** Depth-averaged velocity gradient averaged over each polygon used for the tracer analysis standardized by the mean depth-averaged velocity gradient per polygon (*DAVgrad**). Larger relative gradients would increase the probability that sediment particle velocity would also either increase (indicating a possible erosional zone) or decrease (indicating a possible deposition zone). Zones with significant positive velocity-gradient subareas are denoted with a '+'.

## Acknowledgements

Funding for this effort was provided the Science and

Engineering Program fund provided to the Water Institute of the Gulf by the Baton Rouge Area Foundation and the Louisiana Coastal Protection and Restoration Authority (CPRA). Additional funding was provided through a task order to the Water Institute from the Louisiana CPRA. Ashok Khadka, Hoonshin Jung and Yushi Wang provided invaluable numerical modeling advice in support of this study. Mike Brown, Amy Parry, Cyndhia Ramatchandirane, and Dallon Weathers significantly contributed to the field experiment component of this study. Diana Di Leonardo performed the geological characterization of the analyzed soil samples. Three anonymous reviewers are thanked for their suggested improvements to the manuscript.

## Appendix A. Supplementary data

Supplementary data related to this article can be found at http://dx.doi.org/10.1016/j.ecss.2017.06.004.

## References

Allison, M.A., Meselhe, E.A., 2010. The use of large water and sediment diversions in the lower Mississippi River (Louisiana) for coastal restoration. J. Hydrol. 387, 346–360.
Allison, M.A., Vosburg, B.M., Ramirez, M.T., Meselhe, E.A., 2013. Mississippi River channel response to the Bonnet Carré Spillway opening in the 2011 flood and its implications for the design and operation of river diversions. J. Hydrol. 477, 104–118.
Allison, M.A., Ramirez, M.T., Meselhe, E.A., 2014. Diversion of Mississippi River water and sediment to ameliorate coastal land loss in Louisiana. USA. Water Resour. Manag. 28, 113–4126.
Allison, M.A., Yuill, B.T., Tornqvist, T., Amelung, F., Dixon, T., Erkens, G., Stuurman, R., Jones, C., Milne, G., Steckler, M., Syvitski, J., Teatini, P., 2016. Global risks and research priorities for coastal subsidence. EOS—Trans. Am. Geophys. Union 97 (19), 22–27.
Andrus, T.M., 2007. Sediment Flux and Fate in the Mississippi River Diversion at West Bay: Observation Study (M.S. Thesis). Louisiana State University, Baton Rouge, LA.
Bell, F.W., 1997. The economic valuation of saltwater marsh supporting marine recreational fishing in the southeastern United States. Ecol. Econ. 21 (3), 243–254.
Bianchi, T.S., Allison, M.A., 2009. Large-river delta-front estuaries as natural "recorders" of global environmental change. Proc. Natl. Acad. Sci. 106, 8085–8092.
Blum, M.D., Roberts, H.H., 2009. Drowning of the Mississippi Delta due to insufficient sediment supply and sea level rise. Nat. Geosci. http://dx.doi.org/10.1038/ngeo553.
Boesch, D.F., Turner, R.E., 1984. Dependence of fishery species on salt marshes: the role of food and refuge. Estuaries 7 (4), 460–468.
Britsch, L.D., Dunbar, J.B., 1993. Land loss rates: Louisiana coastal plain. J. Coast. Res. 324–338.
Canestrelli, A., Nardin, W., Edmonds, D., Fagherazzi, S., Slingerland, R., 2014. Importance of frictional effects and jet instability on the morphodynamics of river mouth bars and levees. J. Geophys. Res. Ocean. 119 (1), 509–522.
Coleman, J.M., Gagliano, S.M., 1964. Cyclic sedimentation in the Mississippi River deltaic plain. Trans. – Gulf Coast Assoc. Geol. Soc. 14, 67–80.
Costanza, R., Pérez-Maqueo, O., Martinez, M.L., Sutton, P., Anderson, S.J., Mulder, K., 2008. The value of coastal wetlands for hurricane protection. AMBIO A J. Hum. Environ. 37 (4), 241–248.
Day, J.W., Christian, R.R., Boesch, D.M., Yáñez-Arancibia, A., Morris, J., Twilley, R.R., Naylor, L., Schaffner, L., 2008. Consequences of climate change on the ecogeomorphology of coastal wetlands. Estuaries Coasts 31 (3), 477–491.
Day Jr., J.W., Martin, J.F., Cardoch, L., Templet, P.H., 1997. System functioning as a basis for sustainable management of deltaic ecosystems. Coast. Manag. 25 (2), 115–153.
Edmonds, D.A., Slingerland, R.L., 2007. Mechanics of river mouth bar formation: implications for the morphodynamics of delta distributary networks. J. Geophys. Res. Earth Surf. 112 (F2).
Elias, E., Gelfenbaum, G., Van Ormondt, M., Moritz, H.R., 2011. Predicting sediment transport patterns at the mouth of the Columbia River. Proc. Coast. Sediments 2011, 588–601. http://dx.doi.org/10.1142/9789814355537_0045.
Esposito, C.R., Georgiou, I.Y., Kolker, A.S., 2013. Hydrodynamic and geomorphic controls on mouth bar evolution. Geophys. Res. Lett. 40 (8), 1540–1545.
Gagliano, S.M., Meyer-Arendt, K.J., Wicker, K.M., 1981. Land loss in the Mississippi River deltaic plain. Trans. Gulf Coast Assoc. Geol. Soc. 31, 295–300.
Gaweesh, A., Meselhe, E., 2016. Evaluation of sediment diversion design attributes and their impact on the capture efficiency. J. Hydraul. Eng. http://dx.doi.org/10.1061/(ASCE)HY.1943–7900.0001114.
Kennedy, V.C., Kouba, D.L., 1970. Fluorescent Sand as a Tracer of Fluvial Sediment. United States Geological Survey Professional Paper 562-E. Washington, D.C., p. 18.
Khan, N.S., Horton, B.P., McKee, K.L., Jerolmack, D., Falcini, F., Enanche, M.D., Vane, C.H., 2013. Tracking sedimentation from the historic A.D. 2011 Mississippi River flood in the deltaic wetlands of Louisiana, USA. Geology 41, 391–394.
Kim, W., Mohrig, D., Twilley, R., Paola, C., Parker, G., 2009. Is it feasible to build newland in the Mississippi River Delta? EOS Trans. Am. Geophys. Union 90, 373–374.
Kolker, A.S., Allison, M.A., Hameed, S., 2011. An evaluation of subsidence rates and sea level variability in the northern Gulf of Mexico. Geophys. Res. Lett. 38, L21404,. http://dx.doi.org/10.1029/2011GL049458.
Kolker, A.S., Miner, M.D., Weathers, H.D., 2012. Depositional dynamics in a river diversion receiving basin: the case of the West Bay Mississippi River diversion. Estuar. Coast. Sci. 106, 1–12.
LACPRA (Louisiana Coastal Protection and Restoration Authority), 2012. Louisiana's Comprehensive Master Plan for a Sustainable Coast. State of Louisiana, Baton Rouge, p. 190.
Leeder, M.R., 2009. Sedimentology and Sedimentary Basins: from Turbulence to Tectonics. John Wiley & Sons.
Mariotti, G., Falcini, F., Geleynse, N., Guala, M., Sun, T., Fagherazzi, S., 2013. Sediment eddy diffusivity in meandering turbulent jets: implications for levee formation at river mouths. J. Geophys. Res. Earth Surf. 118 (3), 1908–1920.
Marsh, J.K., Pillsworth, M.W., Kenny, A.J., 1997. Application of innovative fluorescent artificial sand and silt tracers for maintenance dredging optimisation, beneficial use and environmental dredging. In: Proceedings of 2nd Asian and Australasian Ports and Harbours Conference, pp. 173–188.
McComb, P., Black, K., 2005. Detailed observations of littoral transport using artificial sediment tracer, in a high-energy, rocky reef and iron sand environment. J. Coast. Res. 21, 358–373.
Meade, R.H., Yuzyk, T.R., Day, T.J., 1990. Movement and storage of sediment in rivers of the United States and Canada. In: Surface Water Hydrology. Geological Society of America, Boulder, Colorado, pp. 255–280.
Meselhe, E.A., Georgiou, I., Allison, M.A., McCorquodale, J.A., 2012. Numerical modeling of hydrodynamics and sediment transport in lower Mississippi at a proposed delta building diversion. J. Hydrol. 472, 340–354.
Morton, R.A., Barras, J.A., 2011. Hurricane impacts on coastal wetlands: a half-century record of storm-generated features from South Louisiana. J. Coast. Res. 27, 27–43.
Nardin, W., Fagherazzi, S., 2012. The effect of wind waves on the development of river mouth bars. Geophys. Res. Lett. 39 (12).
Nittrouer, J.A., Allison, M.A., Campanella, R., 2008. Bedform transport rates for the lowermost Mississippi River. J. Geophys. Res. 113, F03004. http://dx.doi.org/10.1029/2007JF000795.
Paola, C., Twilley, R.R., Edmonds, D.A., Kim, W., Mohrig, D., Parker, G., Voller, V.R., 2011. Natural processes in delta restoration: application to the Mississippi Delta. Ann. Rev. Mar. Sci. 3, 67–91.
Peyronnin, N., Caffey, R., Cowan Jr., J.H., Dubravko, J., Kolker, A., Laska, S., McCorquodale, A., Melancon Jr., E., Nyman, J.A., Twilley, R., Visser, J., White, J., Wilkins, J., 2016. Building Land in Coastal Louisiana: Expert Recommendations for Operating a Successful Sediment Diversion that Balances Ecosystem and Community Needs. www.MississippiRiverDelta.org/DiversionOpsReport.
Ramirez, M.T., Allison, M.A., 2013. Suspension of bed-material sand over lateral bars in the lower Mississippi River, Southeastern Louisiana. J. Geophys. Research-Earth Surf. Process. 118, 1–20.
Roberts, H.H., 1997. Dynamic changes of the Holocene Mississippi River delta plain: the delta cycle. J. Coast. Res. 13, 605–627.
Roberts, H.H., 1998. Delta switching: early responses to the Atchafalaya River diversion. J. Coast. Res. 14, 882–899.
Roberts, H.H., DeLaune, R.D., White, J.R., Li, C., Sasser, C.E., Braud, D., Weeks, E., Khalil, S., 2015. Floods and cold front passages: impacts on coastal marshes in a river diversion setting (Wax Lake Delta Area, Louisiana). J. Coast. Res. 31 (5), 1057–1068.
Rowland, J.C., Stacey, M.T., Dietrich, W.E., 2009. Turbulent characteristics of a shallow wall-bounded plane jet: experimental implications for river mouth hydrodynamics. J. Fluid Mech. 627, 423–449.
Sharp, J., Little, C., Brown, G., Pratt, T., Health, R., Hubbard, L., Pinkard, F., Martin, K., Clifton, N., Perkey, D., Ganesh, N., 2013. West Bay Sediment Diversion Effects. ERDC/CHL TR-13–15. US Army Corps of Engineers, Engineer Research and Development Center, Vicksburg, MS, p. 274.
Shaw, J.B., Mohrig, D., 2014. The importance of erosion in distributary channel network growth, Wax Lake Delta, Louisiana, USA. Geology 42, 31–34.
Shaw, J.B., Mohrig, D., Wagner, R.W., 2016. Flow patterns and morphology of a prograding river delta. J. Geophys. Research—Earth Surf. http://dx.doi.org/10.1002/2015JF003570.
Syvitski, J.P.M., Saito, Y., 2007. Morphodynamics of deltas under the influence of humans. Glob. Planet. Change 57, 261–282.
Syvitski, J.P.M., Vorosmarty, C., Kettner, A.J., Green, P., 2007. Impact of humans on the flux of terrestrial sediment to the global coastal ocean. Science. http://dx.doi.org/10.1126/science.1109454.
Syvitski, J.P.M., Kettner, A.J., Overeem, I., Hutton, E.W.H., Hannon, M.T., Brakenridge, G.R., Day, J., Vorosmarty, C., Saito, Y., Giosan, L., Nicholls, R.J., 2009. Sinking deltas due to human activities. Nat. Geosci. http://dx.doi.org/10.1038/NGEO629.
Thiessen, A.H., 1911. Precipitation averages for large areas. Mon. Weather Rev. 39

(7), 1082–1089.
USACE, 2012. West Bay 2011 Depth Analysis Process Report. Report to USACE New Orleans District from USACE Mobile District Spatial Data Branch (OP-J).
Wang, H., Steyer, G.D., Couvillion, B.R., Rybczyk, J.M., Beck, H.J., Sleavin, W.J., Meselhe, E., Allison, M.A., Boustany, R.G., Fischenich, C.J., Rivera-Monroy, V.H., 2014. Forecasting landscape effects of Mississippi River diversions on elevation and accretion in Louisiana deltaic wetlands under future environmental uncertainty scenarios. Estuar. Coast. Shelf Sci. 138, 57–68.
Wellner, R., Beaubouef, R., Van Wagoner, J., Roberts, H., Sun, T., 2005. Jet-plume Depositional Bodies—the Primary Building Blocks of Wax Lake Delta, pp. 867–909.
Yuill, B.T., Khadka, A.K., Pereira, J., Allison, M.A., Meselhe, E.A., 2016. Morphodynamics of the erosional phase of crevasse-splay evolution and implications for river sediment diversion function. Geomorphology 259, 12–29.
Yuill, B., Lavoie, D., Reed, D.J., 2009. Understanding subsidence processes in coastal Louisiana. J. Coast. Res. 23–36.